THE JOURNAL OF BIOLOGICAL CHEMISTRY VOL. 288, NO. 6, pp. 3727–3738, February 8, 2013

Deletion of Leucine Zipper Tumor Suppressor 2 (Lzts2) Increases Susceptibility to Tumor Development*[S]

Received for publication, September 7, 2012, and in revised form, December 19, 2012 Published, JBC Papers in Press, December 28, 2012, DOI 10.1074/jbc.M112.417568

Daniel T. Johnson[‡§], Richard Luong[¶], Suk Hyung Lee[‡§], Yue Peng[‡§], Atossa Shaltouki[‡§], Jane T. Lee[‡§], Dong Lin[‖], Yuzhuo Wang[‖], and Zijie Sun[‡§1]

From the Departments of [‡]Urology, [§]Genetics, and [¶]Comparative Medicine, Stanford University School of Medicine, Stanford, California 94305-5328 and the [‖]Department of Cancer Endocrinology, British Columbia Cancer Agency, Vancouver, British Columbia V5Z 1L3, Canada

Background: The leucine zipper putative tumor suppressor 2 (LZTS2) has been speculated to be a tumor suppressor for more than a decade.
Results: Deletion of Lzts2 increases the susceptibility to spontaneous and carcinogen-induced tumor development in mice.
Conclusion: LZTS2 functions as a tumor susceptibility gene.
Significance: Identifying a novel role for LZTS2 in tumorigenesis in a novel mouse model.

Using an *Lzts2* knock-out mouse model, we characterized the biological role of Lzts2 in tumorigenesis. Both heterozygous and homozygous deletion of the *Lzts2*-targeted allele in mice shows an increased incidence in spontaneous tumor development, although Lzts2 homozygous knock-out mice show significantly higher incidences than heterozygous mice. Treatment of *Lzts2*-deficient mice with a carcinogen, *N*-butyl-*N*-(4-hydroxybutyl) nitrosamine, increases the susceptibility to *N*-butyl-*N*-(4-hydroxybutyl) nitrosamine-induced bladder carcinoma development. Examination of human prostate cancer tissue specimens shows a reduction of LZTS2 protein expression in prostate cancer cells. Further analyses of mouse embryonic fibroblasts isolated from Lzts2 knock-out embryos show that loss of Lzts2 enhances cell growth. These data provide the first line of evidence demonstrating that deletion of Lzts2 increases susceptibility to spontaneous and carcinogen-induced tumor development.

The leucine zipper tumor suppressor (*LZTS*) gene family is a group of closely related proteins involved in transcription modulation and cell cycle control (1). *LZTS1*/*FEZ1* is located on human chromosomal region 8p22 and is ubiquitously expressed in normal tissues (2). Deletion of the *Lzts1*/*Fez1* gene in mice results in an increased incidence of both spontaneous and carcinogen-induced tumors (3). The *Lzts2*/*Lapser1* gene was originally identified on the basis of homology with the *Lzts1* gene (1). The human *LZTS2* gene is located on chromosome 10 at 10q24.3, near 10q23.3 where PTEN, a tumor suppressor, was identified (4). It has been shown that both regions are frequently deleted in various human tumors (1), suggesting that additional tumor susceptibility genes may be harbored in this region in addition to PTEN (5). LZTS2 is expressed in most normal tissues, with the highest abundance found in the testis, prostate, and ovary (1, 6). Overexpression of exogenous LZTS2 displayed a repressive effect on cell proliferation in multiple human tumor cell lines (1). The third member of the LZTS family, *LZTS3*, was identified on human chromosome 20p13 and is mainly expressed in the brain and kidney (7).

Significant effort has been spent to investigate the biological role of LZTS2. A protein-protein interaction between LZTS2 and β-catenin has been demonstrated (6). It has been shown that LZTS2 represses β-catenin and T-cell factor/lymphoid enhancing factor-mediated transcription through this interaction (6). A unique Rev-like leucine-rich, CRM1/exportin-regulated nuclear export signal sequence was identified within the carboxyl-terminal region of LZTS2. Through this nuclear export signal site, LZTS2 modulates the nuclear export of β-catenin in a manner dependent on leptomycin B, a CRM1/exportin-α inhibitor. Expression of exogenous LZTS2 can reduce the level of nuclear β-catenin, inhibit the transcriptional activity of β-catenin, and repress cell growth. The effect of LZTS2 on β-catenin was also observed during human adipose tissue differentiation and synaptic cross-talk in neural tissue (8, 9). In addition, LZTS2 has been shown to associate with p80 karatin and inhibit central spindle formation by abrogating microtubule transportation (10, 11).

In this study, we took a loss of function approach to investigate the potential role of LZTS2 in tumorigenesis using an *Lzts2*-deficient mouse strain. Deletion of the *Lzts2* gene in mice shows no obvious pre- or post-natal lethality. Increased spontaneous tumor development was observed in aged *Lzts2* null mice. Homozygous and heterozygous Lzts2 knock-out mice showed increased susceptibility to urinary bladder carcinoma development when treated with *N*-butyl-*N*-(4-hydroxybutyl) nitrosamine (BBN),[2] a chemical carcinogen used to induce uri-

* This work was supported by Public Health Service Grants CA-070297 and CA-151623 from the National Cancer Institute.
[S] This article contains supplemental Figs. S1 and S2.
[1] To whom correspondence should be addressed: Depts. of Urology and Genetics, S287 Grant Bldg., Stanford University School of Medicine, Stanford, CA 94305-5328. Tel.: 650-498-7523; Fax: 650-725-8502; E-mail: zsun@stanford.edu.

[2] The abbreviations used are: BBN, *N*-butyl-*N*-(4-hydroxybutyl) nitrosamine; MEF, mouse embryonic fibroblast; E*n*, embryonic day *n*; X-gal, 5-bromo-4-chloro-3-indolyl-β-D-galactopyranoside; MTS, 3-(4,5-dimethylthiazol-2-yl)-5-(3-carboxymethoxyphenyl)-2-(4-sulfophenyl)-2H-tetrazolium; CM, conditioned medium.

nary bladder cancer. Further analyses of mouse embryo fibroblasts (MEFs) isolated from *Lzts2* knock-out embryos showed that loss of *Lzts2* increases cell proliferation and survival. Reduction of LZTS2 protein expression was observed in human prostate cancer tissues samples. These data provide the first line of evidence demonstrating that LZTS2 functions as a tumor susceptibility gene and plays an important role in tumorigenesis.

EXPERIMENTAL PROCEDURES

Mouse Experiments—The mouse *Lzts2* gene is located on chromosome 19 and was targeted as described previously (12). Briefly, mouse BAC clones (RPCI22129S6/SvEvTac) that contain the mouse *Lzts2* gene were identified by PCR approaches. A PGK-neomycin cassette flanked by *loxP* and *FRT* sites was inserted upstream of exon 2 containing the translation initiating codon, and an additional third *loxP* site was placed downstream of exon 3 using Red/ET recombineering. The linearized target construct was electroporated into 129Svev ES cells; correctly recombined ES clones were identified by PCR using primer sets for the Neo cassette (Neo1, 5′-agcgcatcgccttctatcgccttc-3′), flanking sequences (A2, 5′-tctgagtttgaggcccaccctatgg-3′), and the *loxP* site (5′agggtgttagtttagcaag-3′). Two independent ES clones that were heterozygous for the targeted *Lzts2* alleles were identified. They were injected into C57BL/6 blastocysts and implanted into pseudopregnant recipients. Germ line transmission was achieved by backcrossing male chimeras to wild type C57BL/6J female mice. To generate the whole body knock-outs of *Lzts2* mice, $Lzts2^{floxneo}$ mice were first bred with *β-Actin/Flp* mice to remove the PGK-neomycin cassette (13) and then bred with *EIIa-Cre* mice (14). Mice with *Lzts2* heterozygous allele ($Lzts2^{+/-}$) were backcrossed with C57BL/6J mice for more than four generations before being intercrossed to generate mice homozygous for the null allele ($Lzts2^{-/-}$). To assess Lzts2 on β-catenin-mediated transcription *in vivo*, we obtained Axin2-LacZ reporter mice (strain 009120; The Jackson Laboratory) and crossed them with $Lzts2^{+/-}$ mice to generate $Axin2^{LacZ/+}$:$Lzts2^{+/-}$ mice.

The BBN-induced mouse urinary bladder cancer model was used as follows: 8–10-week-old $Lzts2^{+/+}$, $Lzts2^{+/-}$, and $Lzts2^{-/-}$ littermates were supplied *ad libitum* with tap water containing 0.1% BBN (TCI America, Portland, OR) for 12 weeks followed by tap water without BBN for 2 weeks. Following treatment, the mice were sacrificed and their urinary bladders were collected and preserved in 10% neutral buffered formalin. The urinary bladders were embedded in paraffin, sectioned, and stained with hematoxylin and eosin before being assessed for pathologic abnormalities. Each urinary bladder sample was categorized as "normal," "hyperplasia," or "carcinoma."

Genomic DNA samples isolated from mouse tail tips or embryo yolk sacs were used for genotyping as described in our previous reports (12, 15). Three primers were used to identify wild type and *Lzts2* deleted alleles, including common forward primer, 5′-TACCATCTGAGTTGCTGATTGC-3′; wild type reverse primer, 5′-AGAGAGGAAGGAATGGGAGATC-3′; and deleted reverse primer, 5′-CACAAGGAATGCTCCAACCCTG-3′. PCR was performed as follows: 5 min at 94 °C and then 35 cycles of 94 °C for 45 s, 60 °C for 45 s, and 72 °C for 80 s, followed by a final step at 72 °C for 10 min. $Axin2^{LacZ/+}$ mice were genotyped using the standard $Axin2^{tm1Wbm}$/J genotyping protocol from The Jackson Laboratory (strain 009120). All of the animal experiments performed in this study were approved by the ethics committee of the Administrative Panel on Laboratory Animal Care at Stanford University.

Mouse Embryonic Fibroblasts—Mice heterozygous for the *Lzts2* gene were mated and the female mice were sacrificed at E10.5. The embryos were isolated in cold PBS and then incubated in 500 μl of trypsin (0.25%) for 30 min at 37 °C with intermittent agitation. The embryos were disrupted by pipetting and added to at least a 3× volume of DMEM containing 10% FBS and 1% penicillin/streptomycin. The cells were directly plated into 48-well plates, allowed to adhere overnight, and then used for transient transfection and cell proliferation assays. To determine MEF genotypes, embryo yolk sacs isolated during the dissection were digested and genomic DNA was extracted and used for genotyping with appropriate primers for wild type or mutant *Lzts2* alleles.

Southern, Northern, and Western Blot Analyses—Genomic DNA samples were prepared from yolk sacs of E11.5 mouse embryos and subjected for Southern blot analyses as described previously (12). Northern blot analysis was also carried out using RNA samples isolated from these same embryos. Briefly, 1.5 μg of poly(A) RNA samples were electrophoresed on 1% formalin-denatured agarose gel, blotted onto nylon membrane, and then hybridized with a DNA fragment spanning the junction region between exons 4 and 5 (16). For Western blot analysis, E11.5 mouse embryos were cut into small pieces, homogenized, and then extracted in buffer containing 50 mM Tris-HCl pH 8.0, 1% Nonidet P-40, 150 mM NaCl, 0.5% sodium deoxycholate, 0.1% SDS, 10 μg/ml aprotinin, 10 μg/ml leupeptin, 10 mM phenylmethylsulfonyl fluoride, and 0.5 mM sodium orthovanadate. The whole cell lysates were cleared by centrifugation and supernatants were subjected to SDS-PAGE analysis. The proteins were transferred to nitrocellulose membranes, blocked with 5% milk, and immunoblotted using appropriate primary and species-specific horseradish peroxidase-conjugated secondary antibodies. A polyclonal LZTS2 antibody (6) was used at a 1:50 dilution. The anti-α-tubulin antibody (clone DM1A; Neomarker) and anti-β-catenin antibody (Santa Cruz Biotechnology) were used at 1:1,000 and 1:300 dilutions, respectively.

β-Galactosidase Staining—$Axin2^{+/+}$:$Lzts2^{+/-}$ females were mated with $Axin2^{LacZ/+}$:$Lzts2^{+/-}$ males, and sacrificed at E10.5, and their embryos were dissected and collected in PBS. DNA samples were isolated from yolk sacs for genotyping. The embryos were washed three times with PBS at room temperature, fixed in 0.2% glutaraldehyde fix solution at 4 °C for 30 min, and then washed three times at room temperature for 15 min in washing buffer (0.1 M phosphate buffer, 2 mM $MgCl_2$, 0.02% Nonidet P-40, 0.01% sodium deoxycholate) prior to staining with 1 mg/ml X-gal staining solution (washing buffer with 5 mM potassium ferrocyanide and 5 mM potassium ferricyanide) at room temperature for 45 min. The embryos were then washed three times in washing buffer at room temperature for 10 min each before images were taken. Adult mice were sacrificed and their colons were dissected and frozen in O.C.T. compound

(catalog no. 4583; Sakura-Finetek, Torrance, CA) on dry ice. Cryosections were taken at 10 μm and stored at −80 °C. The slides were fixed in 0.2% glutaraldehyde in PBS for 10 min on ice immediately before use. They were then washed in PBS for 10 min, washed in washing buffer for 10 min, and stained overnight in 1 mg/ml X-gal staining solution at 37 °C. The slides were post-fixed in 4% paraformaldehyde and counterstained with Nuclear Fast Red (catalog no. H3403; Vector Laboratories). The slides were finally washed in water, dehydrated, and then mounted with Permount mounting medium (catalog no. SP15-500; Fisher).

Immunohistochemistry and Immunofluoresence—Human prostate cancer tissue specimens used in this study were collected with informed consent following the protocol approved by the Clinical Research Ethics Board of the University of British Columbia and the British Columbia Cancer Agency. All samples used here were isolated through radical prostatectomy, were pathologically diagnosed prostatic adenocarcinoma, and had not been treated with neoadjuvant hormone therapy. The tissue samples were fixed in 10% neutral buffered formalin and processed to paraffin. Sections were cut at 5-μm intervals, dewaxed in xylene, and hydrated in graded alcoholic solutions. Endogenous peroxidase activity was blocked with 0.5% hydrogen peroxide in methanol for 30 min, then washed with PBS (pH 7.3), and incubated with 5% normal goat serum (catalog no. 0060-01; Southern Biotech, Birmingham, AL) for 30 min. The sections were subsequently incubated with a rabbit polyclonal LZTS2 antibody, a rabbit polyclonal anti-androgen receptor antibody (Affinity BioReagents, Golden, CO), and mouse monoclonal anti-p63 antibody (Santa Cruz Biotechnology). The slides were then incubated with biotinylated anti-rabbit or anti-mouse secondary antibody (BA-1000 or BA-9200; Vector Laboratories) for 1 h and horseradish peroxidase-streptavidin (SA-5004; Vector Laboratories) for 30 min at room temperature and then visualized by DAB kit (SK-4100; Vector Laboratories). All sections used for immunohistochemistry were lightly counterstained with 5% (w/v) Harris hematoxylin. The slides were independently evaluated by two experienced pathologists in blinded analyses. Specimens were graded from no staining (−) to strong staining (+++) as reported previously (17). CD44 immunohistochemistry followed a similar procedure using a rat monoclonal CD44 antibody (Santa Cruz Biotechnology) and a biotinylated anti-rat secondary antibody (BA-9400; Vector Laboratories). For histological analysis of human and mouse tissues, 5-μm serial sections were processed from xylene to water through a decreasing ethanol gradient, stained with hematoxylin and eosin, and processed back to xylene through an increasing alcohol gradient. Coverslips were mounted using Permount mounting medium (catalog no. SP15-500; Fisher). For immunofluorescence, MEFs or other human cell lines were plated onto chamber slides, cultured for 24 h, and then fixed for 10 min with 4% paraformaldehyde. The cells were then permeabilized and blocked for nonspecific sites with 0.04% Triton X-100, 5% goat serum, PBS buffer for 30 min and then incubated with appropriate primary antibodies overnight at 4 °C. The cells were washed three times followed by incubation with appropriate secondary antibodies. The samples were also counterstained with 1 ng/ml DAPI.

Cell Cultures, Lentivirus Production, and Transient Transfections—LNCaP and LAPC4 prostate cancer cell lines were maintained as described previously (18). Transient transfections were carried out using a Lipofectamine 2000 kit (catalog no. 11668-027; Invitrogen). Approximately 1.5×10^4 cells were seeded into a 48-well plate 16 h before transfection. Approximately 300 ng of total plasmid DNA and 0.5 μl of Lipofectamine 2000 per well were used in the transfection as previously described (6). Lentiviruses were generated by cotransfection of pLenti-FLAGLZTS2, pCMV-dR8.91, and pMD2.G-VSVG into HEK293 cells at a ratio of 3:2:1 using a Lipofectamine 2000 kit (Invitrogen) as described previously (19, 20). The media were replaced at 6 h post-transfection and then collected 36–40 h later. The viral supernatant was centrifuged briefly to remove cellular debris and stored at −80 °C. Lentivirus infection was carried out in the presence of 6 mg/ml Polybrene and then selected with puromycin (Sigma) after 48 h.

Cell Proliferation Assays—Approximately 2000 cells/well were plated and cultured in the presence of either Wnt3a-CM or L-CM, which was prepared as described previously (21), and then harvested at different time points. Proliferation assays were carried out using the MTS tetrazolium kit (Promega, Madison, WI). Cell numbers were determined by absorbance at 490 nm as suggested by the manufacturer. For the colony formation assay, MEFs, LNCaP, or LAPC4 cells were plated in 6-well plates (500–1000 cells/well) for 24 h and then maintained in Wnt3a-CM or in L-CM for 10–12 days. The cells were stained with crystal violet (Sigma), and the colonies containing more than 50 cells were counted. Colony assays were performed a minimum of three times, and the results are reported as the means of three experiments.

Luciferase Reporter Assays—Mouse embryonic fibroblasts were isolated and maintained as described previously (22). Wnt3a-conditioned media or L-media were prepared according to the previous report (21). Transient transfection and luciferase assays were performed using Topflash (pGL3-OT, OT-Luc) and Foflash (pGL3-OF, OF-Luc) luciferase reporters as described previously (6). The luciferase activity from individual transfections was normalized by β-galactosidase activity in the same samples and reported as relative light units. The relative light units were determined from three independent transfections. The results are presented as the means ± S.E. of the triplicate transfections.

Statistical Analyses—We presented the data as the means ± S.D. We made comparisons between groups, using a two-sided Student's t test. $p < 0.05$ and $p < 0.01$ were considered significant.

RESULTS

Disruption of the Lzts2 Gene in Mouse ES Cells and Embryos—The LZTS2 protein belongs to the LZTS family and has been speculated as a tumor suppressor for more than a decade (1, 6). In this study, we took a loss of function approach to directly address the important role of LZTS2 in tumorigenesis using an *Lzts2*-deficient mouse strain. The Lzts2 protein is highly conserved between humans and mice (Fig. 1*A*). We constructed a "*floxed*" targeting allele in the mouse *Lzts2* locus using targeted homologous recombination approaches (Fig. 1*B*). *Lzts2* con-

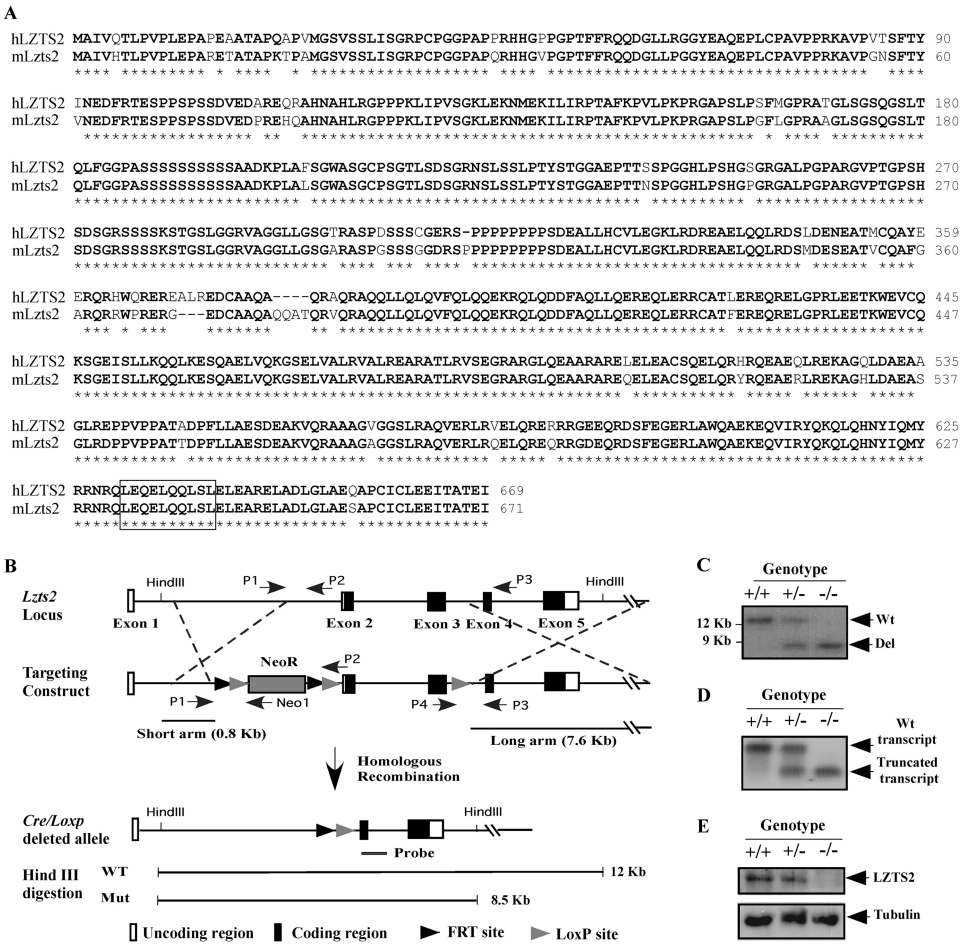

FIGURE 1. **Disruption of the *Lzts2* gene in mouse ES cells and embryos.** *A*, alignment of human and mouse LZTS2 protein sequences is shown. Identical amino acids are in *bold type* and marked with *asterisks*. The nuclear export signal is *boxed*. *B*, the targeting construct used to disrupt the *Lzts2 gene* in ES cells. A PGK-neomycin cassette flanked by *loxP* and *FRT* sites was inserted upstream of exon 2 (which contains the translation initiating codon). A third *loxP* site was placed downstream of exon 3 using Red/ET recombineering. The hypothetical crossovers between the endogenous *Lzts2* allele and the targeting construct are indicated by the *dashed lines*. Correctly recombined ES clones were identified by PCR using primer sets for the Neo cassette (*Neo1*), flanking sequences (*P2*), and the downstream *loxP* site (*P3*). *C*, Southern blotting of E11.5 embryos using a ^{32}P-labeled probe from exon 4. *D*, Northern blotting of total RNA from E11.5 embryos using a ^{32}P-labeled probe covering the junction region of exons 4 and 5. *E*, Western blotting of total cell lysates from E11.5 mouse embryos analyzed with an LZTS2 antibody.

ventional knock-out mice were produced by mating *Lzts2 floxed* mice with *β-Actin/Flp* transgenic mice to remove the PGK-neomycin cassette (13) and then subsequently breeding with *EIIa-Cre* mice (23) to delete the coding region of *Lzts2* between amino acids 1 and 357 (Fig. 1*B*). Further intercrossing between *Lzts2* heterozygous mice ($Lzts2^{+/-}$) produced homozygous knock-out mice ($Lzts2^{-/-}$). Genotypes of Lzts2 knock-out mice were analyzed using mouse genomic DNA samples isolated from E11.5 embryos by Southern blot with a probe derived from exon 4 (Fig. 1*B*). An 8.5- or 12.5-kb fragment corresponding with the deleted or wild type allele was detected in different genotypes of embryos accordingly (Fig. 1*C*). Using specific primers (*P1*, *P3*, and *P4* in Fig. 1*B*), we further assessed the genotypes of embryos using genomic PCR analysis (data not shown). Total RNA samples were isolated from E11.5 embryos and analyzed by Northern blot using a probe spanning the junction region between exons 4 and 5 (Fig. 1*D*). Finally, we evaluated Lzts2 protein expression using an anti-Lzts2 antibody in Western blot analyses. The Lzts2 protein was detected in wild type and, to a lesser extent, in heterozygous embryos but was absent in *Lzts2* null embryos (Fig. 1*E*). We also examined Lzts2 expression in adult knock-out mouse tissues and observed a similar expression pattern (data not shown). Taken together, the above data demonstrate that the expression of the Lzts2 protein was disrupted in *Lzts2* null mice.

Lzts2 Null Mice Develop Spontaneous Tumors at Old Ages—Mice heterozygous and homozygous for deleted *Lzts2* allele ($Lzts2^{+/-}$ and $Lzts2^{+/-}$) were viable, fertile, and born at the expected Mendelian ratios. We observed abnormalities of the kidney and urinary tract in some $Lzts2^{-/-}$ mice starting at early embryonic development, which included unilateral kidney hydronephrosis, mildly dilated and shortened ureter, duplicated kidney, and duplicated ureters (12). One of the central reasons for generating *Lzts2* knock-outs was to assess the potential role of Lzts2 in tumorigenesis. Through efforts to systemically analyze *Lzts2* knock-out mice, we observed an increased rate of spontaneous tumor formation in both heterozygous and homozygous Lzts2 knock-out mice after 12 months of age (Table 1). Multiple neoplasms were observed in a 14-month-old $Lzts2^{-/-}$ male mouse, including in the pancreas

TABLE 1
Development of spontaneous tumors in Lzts2 knock-out mice

Genotype	Number of mice			Mice with tumors (tumor incidence)		
	Male	Female	Total	Male	Female	Total
Lzts2$^{+/+}$						
<12 months	21	8	29	0	0	0
>12 months	17	16	33	1/17 (5.9%)	2/16 (12.5%)	3/33 (9.1%)
Lzts2$^{+/-}$						
<12 months	14	13	27	0	0	0
>12 months	11	13	24	2/11 (18.1%)	2/13 (15.4%)	4/24 (16.7%)[a]
Lzts2$^{-/-}$						
<12 months	9	8	17	0	0	0
>12 months	14	17	31	5/14 (35.7%)	6/17 (35.3%)	11/31 (35.5%)[a]

[a] *Lzts2*$^{+/-}$ mice have a higher tumor incidence than wild type littermates ($p < 0.01$).

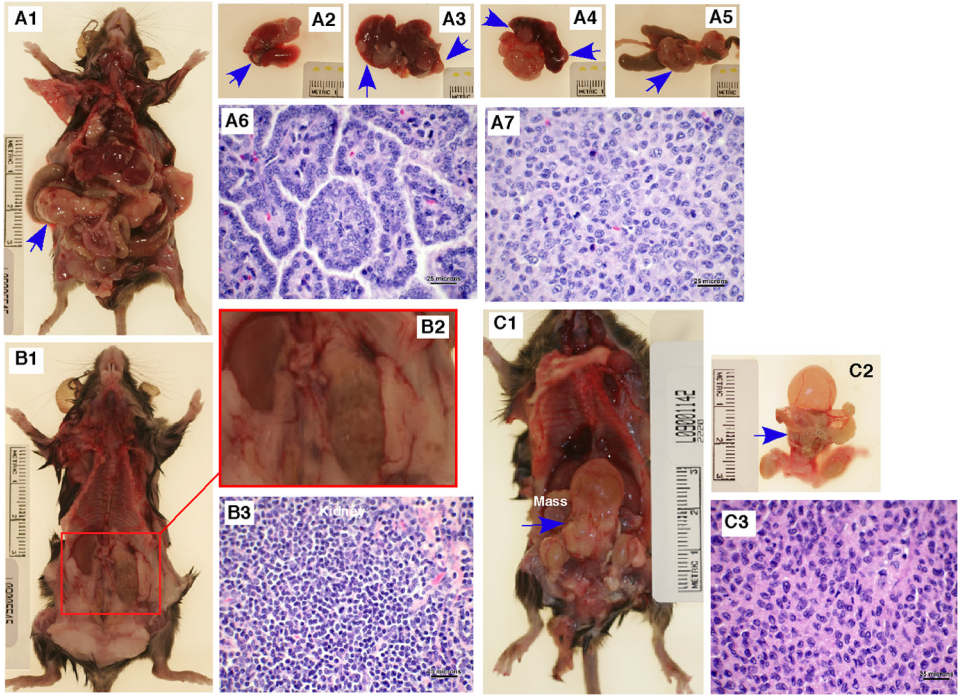

FIGURE 2. **Development of spontaneous tumors in Lzts2 null mice.** *A*, a 14-month-old male *Lzts2*$^{-/-}$ mouse was sacrificed, and necropsy showed multiple nodular masses in different organs (*arrows*), including the pancreas (*panel A1*), lung (*panel A2*), liver and gallbladder (*panel A3*), spleen (*panel A4*), and intestine and mesenteric lymph node (*panel A5*). Histological analyses of masses in the lung suggest pulmonary carcinoma (*panel A6*) and histiocytic sarcoma in the remaining affected organs (*panel A7*) are also shown. *B*, a 16-month-old female *Lzts2*$^{-/-}$ mouse was grossly examined, revealing lymphadenopathy of the both mandibular and sublumbar lymph nodes and left renomegaly (*panels B1* and *B2*). Microscopic analysis confirmed that the lymph nodes and left kidney were affected by multicentric lymphoma (*panel B3*), with additional microscopic involvement of the right kidney, retroperitoneum adjacent to ureters and aorta, salivary glands, liver, and lung. *C*, necropsy of a 17-month-old male *Lzts2*$^{-/-}$ mouse showed a focally extensive, pale tan partially multilobulated mass in the region of the prostate gland and trigone of the urinary bladder (*panels C1* and *C2*). Histological analysis of the mass suggests a primary histiocytic sarcoma of the prostate gland (*panel C3*).

(Fig. 2, *panel A1*), lung (Fig. 2, *panel A2*), liver and gallbladder (Fig. 2, *panel A3*), spleen (Fig. 2A4), and intestine and mesenteric lymph node (Fig. 2, *panel A5*). The tumor in the lung was diagnosed as a primary pulmonary carcinoma (Fig. 2, *panel A6*), whereas a primary histiocytic sarcoma was diagnosed in the mesenteric lymph node (Fig. 2, *panel A7*), with secondary metastases to the pancreas, spleen, liver, gallbladder, and intestines. A 16-month-old female *Lzts2*$^{-/-}$ mouse was grossly examined, revealing lymphadenopathy of the both mandibular and sublumbar lymph nodes and left renomegaly (Fig. 2, *panels B1* and *B2*). Microscopic analysis confirmed that the lymph nodes and left kidney were affected by multicentric lymphoma (Fig. 2, *panel B3*), with additional microscopic involvement of the right kidney, retroperitoneum adjacent to ureters and aorta, salivary glands, liver, and lung. In a 16-month-old male *Lzts2*$^{-/-}$ mouse, a prostatic mass was observed on gross examination (Fig. 2, *panels C1* and *C2*) that was confirmed histologically as a primary histiocytic sarcoma (Fig. 2, *panel C3*). Incidences of spontaneous tumor development in heterozygous and homozygous *Lzts2* knock-out mice were 16.7 and 35.5%, respectively, and significantly higher than in wild type control littermates (9.1%), respectively (Table 1). We did not observe a significant difference in spontaneous tumor development between male and female *Lzts2*-deficient mice.

Loss of Lzts2 Expression Enhances Cell Proliferation—Development of spontaneous tumors in *Lzts2*-deficient mice provides the first line of evidence demonstrating that the deletion of Lzts2 results in tumor-prone phenotypes, which also implies a role of Lzts2 in regulating cell proliferation. In this regard, we assessed the potential effects of LZTS2 on cell growth and sur-

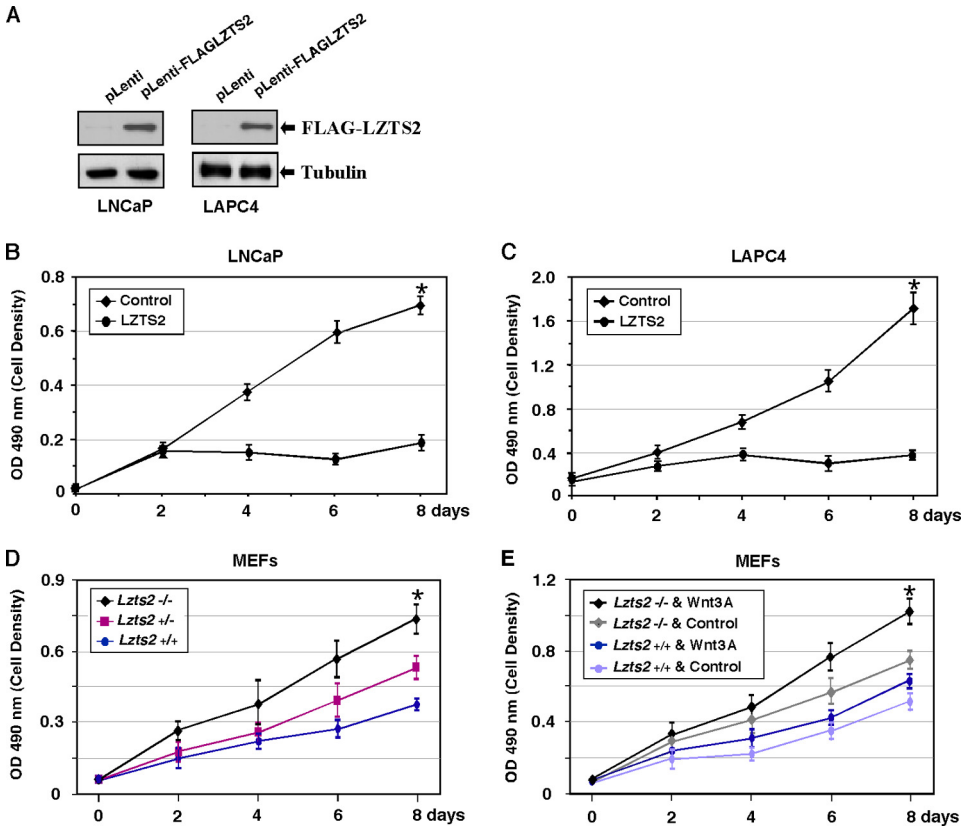

FIGURE 3. **Effects of Lzts2 in cell proliferation and survival.** *A*, Western blot analysis of FLAG-LZTS2 expression in LNCaP or LAPC4 cells after infection with pLenti-FLAGLZTS2 or control lentiviruses. The same blots were probed with an anti-tubulin antibody as a control. *B*, LNCaP cells were seeded into 96-well plates after 6 h of infection with LZTS2 expression lentiviruses. Cell growth was measured every other day by MTS assay. The data represent the means ± S.D. of three independent experiments. *C*, identical experiments performed in LAPC4 cells. *D*, MTS cell proliferation assay using E10.5 MEFs isolated from *Lzts2*. heterozygous intercrosses (+/+, $n = 4$; +/−, $n = 4$; −/−, $n = 3$). *E*, both $Lzts2^{+/+}$ and $Lzts2^{-/-}$ MEFs were incubated in either Wnt3a-CM or control medium and tested by MTS assays.

vival. We first tested the effect of LZTS2 in two prostate cancer cell lines, LNCaP and LAPC4, by transduction with FLAG-tagged LZTS2 expression lentiviruses (Fig. 3*A*). LNCaP cells with exogenous LZTS2 expression grew more slowly than control cells that were infected with control viruses ($p < 0.05$), suggesting a repressive role of LZTS2 in the growth of LNCaP cells (Fig. 3*B*). In addition, overexpression of exogenous LZTS2 protein also significantly inhibited LNCaP cell growth in colony formation assays (data not shown). Using similar experimental approaches, we also demonstrated the repressive role of LZTS2 in LAPC4 cell growth (Fig. 3*C*). Next, we assessed the role of endogenous Lzts2 protein in cell growth and survival. *Lzts2* heterozygous mice were mated, and the female mice were sacrificed at 10.5 days post coitus. The embryos were isolated for making MEFs from *Lzts2*-deficient mice (15, 24). We then used MEFs to further evaluate the repressive role of LZTS2 in cell growth and survival. A significant increase in cell growth was observed in $Lzts2^{-/-}$ MEFs when compared with wild type or heterozygous MEFs ($p < 0.05$; Fig. 3*D*). Because LZTS2 has been identified as a regulator of Wnt and β-catenin signaling pathways, we further explored the effect of Wnt3a conditioned medium on cell proliferation in *Lzts2*-deficient MEFs. In the presence of Wnt3a-conditioned media, *Lzts2* null MEFs appear to have a higher growth rate than in the presence of control media (Fig. 3*E*). The enhancement of Wnt3a conditional media is more pronounced in *Lzts2* null MEFs than wild type cells at day 8 ($p < 0.05$; Fig. 3*E*). These results further suggest that deletion of *Lzts2* enhances Wnt3a-mediated cell growth in *Lzts2* null MEFs.

Lzts2-deficient Mice Are More Susceptible to Carcinogen Induction—BBN is a well established carcinogen that has been frequently used in rodents to induce the development of urinary bladder cancer, which bears significant histopathological and molecular similarities to the human disease (25). Therefore, the BBN-induced bladder cancer model has been frequently used to characterize the tumorigenic process of urinary bladder cancer (26). In this study, we assessed the carcinogenic effect of BBN in *Lzts2*-deficient mice to determine whether Lzts2 modulates carcinogen-induced malignancy development. All of the mice were treated with 0.1% BBN in their drinking water for 12 weeks and sacrificed 2 weeks after ending BBN treatment. We observed the pathological changes of simple hyperplasia (10 of 21, 47.6%) and *in situ* carcinoma (2 of 21, 9.5%) in $Lzts2^{+/+}$ control mice (Table 2). However, hyperplasia occurred in 12 of 28 (42.9%) $Lzts2^{+/-}$ and 8 of 26 (30.7%) $Lzts2^{-/-}$ mice. Importantly, a significant increase of transitional cell carcinomas was observed in both $Lzts2^{+/-}$ (9 of 28, 32.1%) and $Lzts2^{-/-}$ (10 of 26, 38.5%) mice. A typical series of pathological changes reflecting the progression of invasive transitional cell carcinoma development was observed in $Lzts2^{-/-}$ mice (Fig. 4, *B–E*). We observed invasive transitional cell carcinomas in 6 of the 26 $Lzts2^{-/-}$ mice but none in

TABLE 2
Development of inducible tumors in Lzts2 knock-out mice

Genotype	Normal	Hyperplasia	Transitional cell carcinomas				
			Total	*In situ*	Noninvasive	Invasive	Total
Lzts2$^{+/+}$	9/21 (42.9%)	10/21 (47.6%)	2/21 (9.5%)	2	0	0	21
Male	4	5	1 (10%)	1	0	0	10
Female	5	5	1 (9.1%)	1	0	0	11
Lzts2$^{+/-}$	7/28 (25.0%)	12/28 (42.9%)	9/28 (32.1%)[a]	5	4	0	28
Male	3	6	9 (50%)[b]	5	4	0	18
Female	4	6	0	0	0	0	10
Lzts2$^{-/-}$	8/26 (30.7%)	8/26 (30.7%)	10/26 (38.5%)[a]	2	2	6	26
Male	2	6	8 (50%)[b]	0	2	6	16
Female	6	2	2 (20%)[a]	2	0	0	10

[a] *Lzts2*$^{+/-}$ or *Lzts2*$^{-/-}$ mice have a higher tumor incidence than wild type littermates ($p < 0.01$).
[b] *Lzts2*$^{+/-}$ or *Lzts2*$^{-/-}$ male mice have a higher tumor incidence than age and sex-matched wild type littermates ($p < 0.01$).

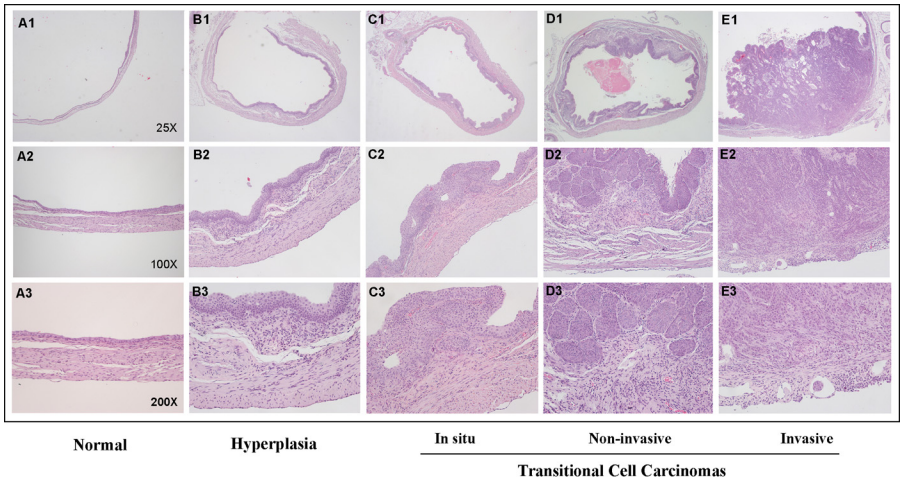

FIGURE 4. **Histologic analysis of *Lzts2*-deficient murine urinary bladder after BBN treatment.** Hematoxylin- and eosin-stained sections of representative samples of normal urothelium (*A1–3*), hyperplasia (*B1–3*), carcinoma *in situ* (*C1–3*), and noninvasive (*D1–3*)/invasive (*E1–3*) transitional cell carcinoma. The images were taken at 25×, 100×, or 200× magnification.

Lzts2$^{+/-}$ or *Lzts2*$^{+/+}$ littermates (Table 2). These results suggest that LZTS2 deletion increases the susceptibility to BBN-induced urothelial cell carcinoma initiation and progression.

Expression of LZTS2 Is Reduced in Prostate Cancer Specimens—In this study, we also examined the expression and cellular localization of the LZTS2 protein in human prostate cancer samples. Adjacent serial sections from the same tissue block were stained with antibodies against androgen receptor, LZTS2, or p63. Androgen receptor staining, a prostatic epithelial marker, was seen exclusively in the nucleus of luminal cells in both normal and malignant prostatic glands (Fig. 5, *A*, *D*, and *G*). The p63, a homologue of p53, selectively stained in prostatic basal cells as reported previously (27). Because basal cells are absent in malignant prostatic glands, the presence of p63 is a useful marker to distinguish normal from tumor sections (*red arrows versus green arrows* in Fig. 5, *B*, *E*, and *H*). Positive staining of LZTS2 was observed in the cytoplasm of luminal cells, and there was no or very weak staining in stromal elements (Fig. 5, *C*, *F*, and *I*). There is no specific staining in control samples stained with normal IgG staining (data not shown). Importantly, the intensity of LZTS2 staining in malignant prostatic glands appears significantly weaker than in normal, p63-positive glands (*green arrows versus red arrows* in Fig. 5, *C*, *F*, and *I*). We semi-quantitatively scored the intensity of staining with each antibody in normal or malignant sections as reported previously (17) (Table 3). Decreased LZTS2 expression was observed in 13 of 17 prostate cancer samples ($p < 0.05$). These data suggest that LZTS2 is abnormally expressed in prostate cancer specimens and also confirms the cytoplasmic localization of endogenous LZTS2 protein in human prostate epithelial cells.

Loss of Lzts2 Expression Alters the Cellular Localization and Activity of β-Catenin—Previously, we have shown that LZTS2 functions as a β-catenin-interacting protein and regulates the cellular localization and activity of β-catenin in human cancer cell lines (6). We took advantage of our newly generated *Lzts2* knock-out mice to further assess the role of endogenous Lzts2 in the regulation of β-catenin cellular localization and activity in a more biologically relevant system. We isolated MEFs from different genotypes of *Lzts2* knock-out littermates. We first analyzed the expression of Lzts2 in whole cell lysates prepared from the different genotype MEFs. The expression of Lzts2 proteins was only detected in MEFs isolated from wild type and heterozygous embryos, but not MEFs from *Lzts2* null embryos in Western blotting assays (Fig. 6*A*). We next evaluated the expression and cellular localization of β-catenin in the above MEFs. Although there is slightly elevated total β-catenin in *Lzts2* null MEFs, a notable increase of nuclear β-catenin was observed in the nuclear extract of *Lzts2* null MEFs (Fig. 6*B*). These data suggest that the deletion of endogenous LZTS2 proteins results in accumulated nuclear β-catenin, which is consistent with our previous observation that LZTS2 regulates the

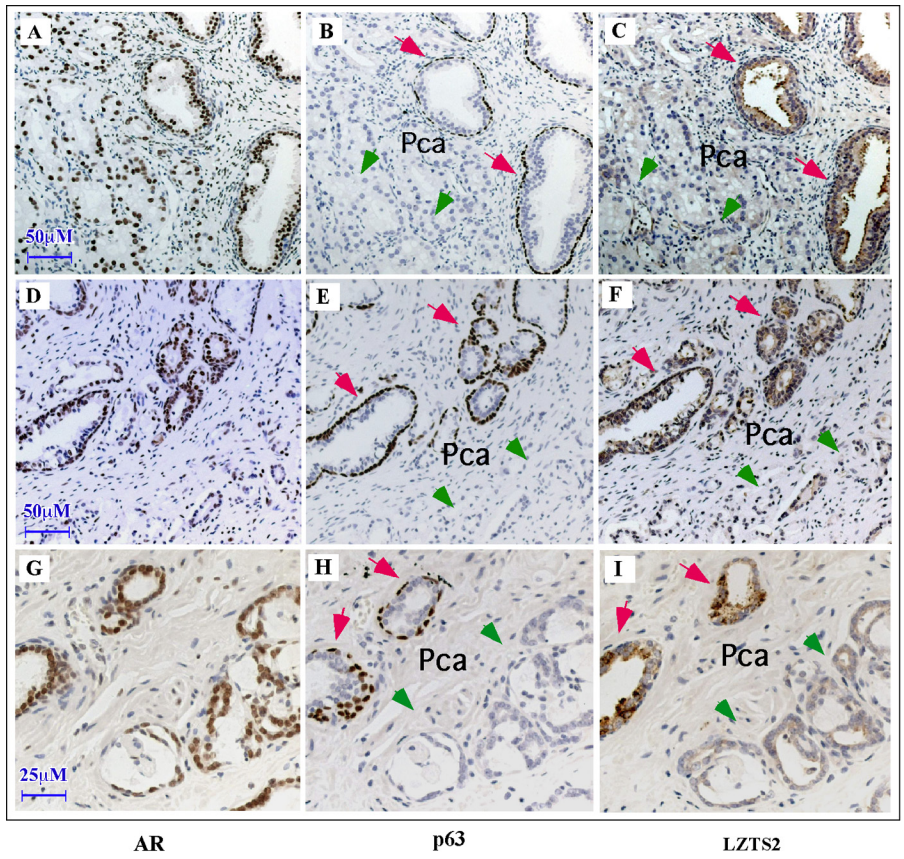

FIGURE 5. **Reduction of LZTS2 expression in human prostate cancer samples.** Three sets of human prostate tissue samples were stained with antibodies against androgen receptor (*AR*) (*A*, *D*, and *G*), p63 (*B*, *E*, and *H*), or LZTS2 (*C*, *F*, and *I*). All sections used for immunohistochemistry were lightly counterstained with 5% (w/v) Harris hematoxylin. LZTS2 staining is much weaker in malignant glands (*green arrows*) *versus* normal glands (*red arrows*).

TABLE 3
Expression of LZTS2, p63, and androgen receptor in normal and malignant prostate tissues

	Normal			PCa		
Case no.	*LZTS2*	*p63*	Androgen receptor	*LZTS2*	*p63*	Androgen receptor
H34	++	++	++	+	−	+
H40	+[a]	++	++	±	−	+
H50	++	++	++	+	−	++
AB23	++	+	++	+	−	++
3034	++	++	++	±	−	++
334542	++	++	++	±	−	++
338543	++	++	++	+	−	++
346919	++	++	++	++	−	++
345409A	No tissue	No tissue		±	−	++
329349	No tissue	No tissue		+	−	++
S09003	++	++	++	+	−	++
S09012	++	++	++	−	−	++
S09017	+	++	++	±	−	+
S09023	++	++	++	+	−	++
S09012	++	++	+	−	−	++
S09017	+	++	++	+	−	+
S09023	++	++	+	+	−	++

[a] Atrophic benign tissues.

nuclear export of β-catenin through its nuclear exporting signal (6). Using immunofluorescence approaches, we further examined the subcellular localization of endogenous Lzts2 in the above MEFs. Most of the Lzts2 proteins were located in the cytoplasm, surrounding the nuclear envelope in wild type MEFs, but no staining was observed in *Lzts2* null MEFs (Fig. 6*C*). These data confirm our previous observation that Lzts2 is primarily localized in the cytoplasm (6). We next examined β-catenin-mediated transcription in *Lzts2* MEFs. We transfected Topflash (OT-Luc) and Foflash (OF-Luc) luciferase reporters into the above MEFs, and cultured cells in the presence of Wnt3a-CM or L-CM, as a control (21). As shown in Fig. 6*D*, Wnt3a-CM showed a highly pronounced induction of luciferase activity by the Topflash promoter/reporter in two *Lzts2* null MEF lines compared with wild type or $Lzts2^{+/-}$ MEFs. There was no or little activity in the samples treated with L-CM or those transfected with the Foflash promoter/reporter (data not shown). We also examined endogenous β-catenin downstream target genes using *Lzts2* MEFs. An increase in cyclin D1, c-Jun, and Axin2 expression was observed in *Lzts2*

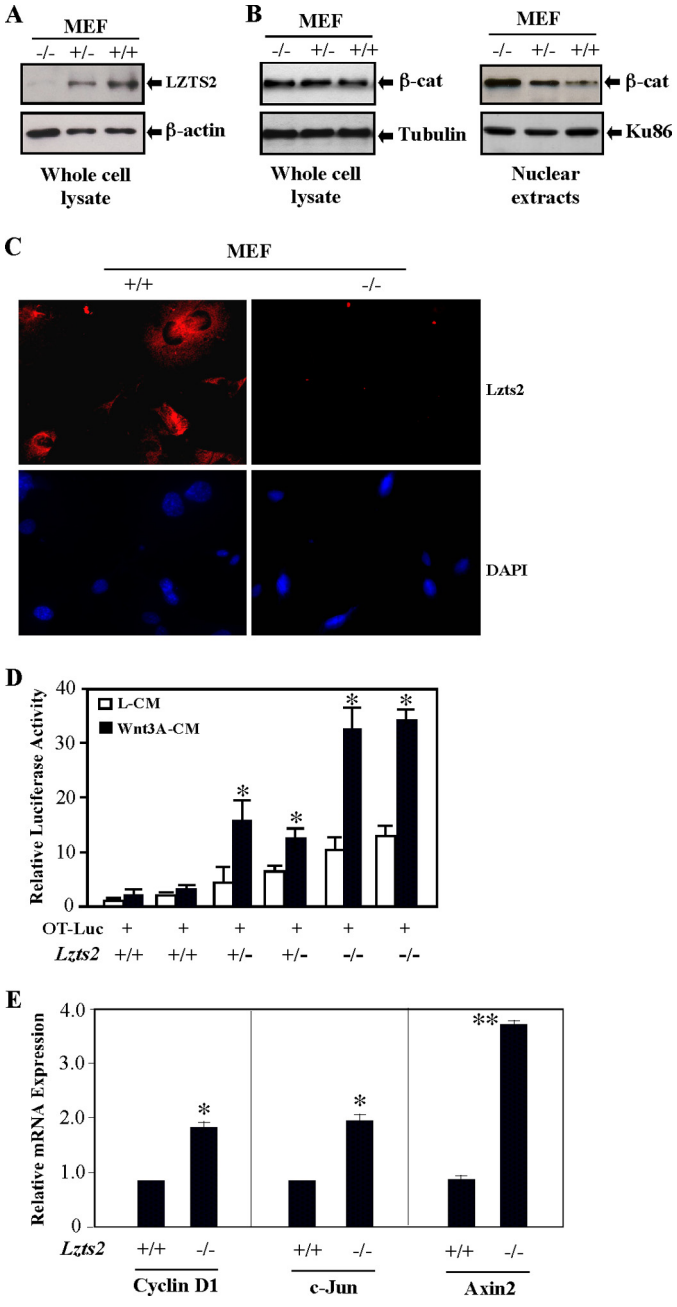

FIGURE 6. **Cellular localization and activity of β-catenin in Lzts2 null MEFs.** *A*, MEFs were prepared from different genotype embryos at E10.5. Whole cell lysates were analyzed by Western blotting assays with either LZTS2 or β-actin antibody. *B*, either whole cell lysates or nuclear extracts were isolated from different genotype MEFs and analyzed by Western blotting assays for either β-catenin (*β-cat*), Ku86, or tubulin. *C*, both wild type and Lzts2 null MEFs were fixed and incubated with the anti-LZTS2 antibody followed by a second antibody conjugated with rhodamine (*red*). The nuclei were counterstained with DAPI (*blue*). *D*, luciferase assay of different genotype MEFs cultured in either Wnt3a-CM or L-CM. Luciferase activity is reported as relative light units (luciferase/β-galactosidase) and represented as the means ± S.D. *E*, quantitative RT-PCR assays were performed to detect mRNA levels of the endogenous beta-catenin downstream target genes Cyclin D1, c-Jun, and Axin2. The experiments were repeated three times using independent cDNA samples from wild type and Lzts2 null MEFs. The relative mRNA levels from each sample are presented as the mean ± S.E. of the triplicate reactions. A statistically significant difference (*, $p < 0.05$; **, $p < 0.01$) was observed between wild type and Lzts2 null MEFs for each target gene.

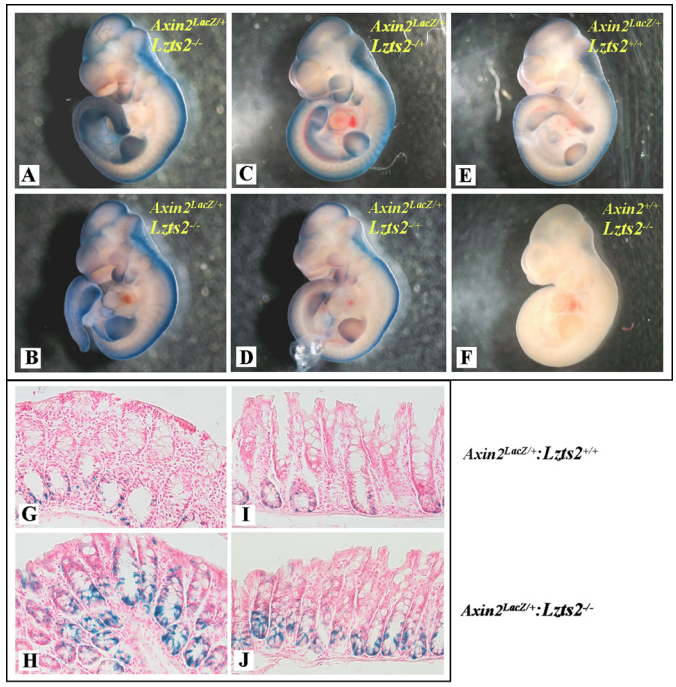

FIGURE 7. **Loss of Lzts2 alters β-catenin activity in mice.** β-Galactosidase staining of E10.5 embryos using the Wnt activity reporter, $Axin2^{LacZ/+}$ (*A–F*). Increased staining was observed dorsally and in the forebrain, midbrain, hindbrain, and mandibular branches of $Axin2^{LacZ/+}$:$Lzts2^{-/-}$ (*A* and *B*) and $Axin2^{LacZ/+}$:$Lzts2^{+/-}$ (*C* and *D*) embryos as compared with $Axin2^{LacZ/+}$:$Lzts2^{+/+}$ (*E* and *F*) embryos. *G–J*, increased Wnt activity was also observed in the intestinal crypts of the colons of adult $Axin2^{LacZ/+}$:$Lzts2^{-/-}$ mice (*H* and *J*) compared with $Axin2^{LacZ/+}$:$Lzts2^{+/+}$ mice (*G* and *I*).

null MEFs in comparison with wild type MEFs (Fig. 6*E*). Taken together, these data indicate that the deletion of Lzts2 expression regulates the cellular localization and activity of endogenous β-catenin in MEFs, which confirms our previous observation in human cancer cells.

Lzts2 Alters β-Catenin-mediated Transcriptional Activity in Vivo—To further examine the role of Lzts2 in regulating Wnt/β-catenin signaling, we crossed $Lzts2^{+/-}$ mice with the $Axin2^{LacZ/+}$ reporter strain to generate *Lzts2* knock-out and *Axin2* reporter compound mice. Axin2 is a downstream target of the canonical Wnt signaling pathway and therefore has been used to assess Wnt activity. In the $Axin2^{LacZ/+}$ reporter strain, the endogenous *Axin2* gene is replaced with a NLS-LacZ reporter gene under the control of the endogenous Axin2 promoter/enhancer (28). We first assessed *Axin2LacZ* reporter expression during embryonic development. β-Galactosidase staining was detected at E10.5 in $Axin2^{LacZ/+}$:$Lzts2^{+/-}$ and $Axin2^{LacZ/+}$:$Lzts2^{-/-}$ embryos (Fig. 7, *A--D*). The staining in $Axin2^{LacZ/+}$:$Lzts2^{-/-}$embryos generally appears stronger than in $Axin2^{LacZ/+}$:$Lzts2^{+/-}$ embryos (Fig. 7, *A* and *B versus C* and *D*). The areas of intense staining include the forebrain, midbrain, hindbrain, and mandibular brachial arches. The staining displayed widespread dorsal expression, including the tail bud. Craniofacial staining was apparent. Interestingly, the embryo forelimbs and hindlimbs also displayed significant staining. This staining pattern is very similar to endogenous Lzts2 expression in mouse embryos (12), suggesting that deletion of Lzts2 in mouse embryos enhances endogenous β-catenin downstream target expression. There is visible staining in

Axin2$^{LacZ/+}$:*Lzts2*$^{+/+}$ embryos (Fig. 7*E*), but no staining is observed in wild type control embryos (Fig. 7*F*). We additionally utilized the *Axin2*^{LacZ} reporter to examine Wnt activity in adult mice. It is well established that β-catenin-mediated activity is detectible in the intestinal crypts of adult mice using the Axin2 Lacz reporter (28). Therefore, we examined β-galactosidase activity in adult mouse colon tissues from *Axin2*$^{LacZ/wt}$:*Lzts2*$^{+/+}$ and *Axin2*$^{LacZ/wt}$:*Lzts2*$^{-/-}$ mice. Faint but clear β-galactosidase activity is shown in the crypts of colon sections from *Axin2*$^{LacZ/wt}$:*Lzts2*$^{+/+}$ mice (Fig. 7, *G* and *I*). β-Galactosidase staining of *Axin2*$^{LacZ/wt}$:*Lzts2*$^{-/-}$ mice tissue shows a similar pattern, but with a much stronger signal than *Axin2*$^{LacZ/wt}$:*Lzts2*$^{+/+}$ mice (Fig. 7, *H* and *J*). We also examined the expression of CD44, a downstream target gene of β-catenin, in the crypts of the colon and observed more intensive staining in *Lzts2* knock-out mice (supplemental Fig. S2). Taken together, these results show the enhancement of Wnt/β-catenin signaling caused by Lzts2 deletion *in vivo*.

DISCUSSION

In this study, we investigated a long unanswered question regarding the role of LZTS2 in tumorigenesis. LZTS2, also named LAPSER, was originally identified as a homologue of FEZ1/LZTS1 based on their closely related sequences (1). Although a potential role of LZTS2 as a tumor suppressor has been speculated for more than a decade, there is no evidence directly demonstrating the role of LZTS2 in tumor initiation or progression. To address this question, we generated *Lzts2*-deficient mice and analyzed them by a watchful waiting approach. We observed an increase in spontaneous tumor development in both aged *Lzts2* heterozygous (16.7%) and homozygous (35.5%) knock-out mice in comparison with wild type littermates (9.1%). Interestingly, all mice that developed spontaneous tumors were more than 12 months old. There is no significant difference in the average mouse ages of tumor onset between the different genotype mice (data not shown). The most frequent malignancies observed in Lzts2-deficient mice include lymphomas, adenocarcinomas in digestive organs, histiocytic sarcomas, and pulmonary carcinomas. Carcinomas in the ovary, mammary glands, or prostate were also observed in female or male *Lzts2*-deficient mice, respectively. These data provide the first line of evidence linking Lzts2 deletion to a tumor-prone phenotype in mice.

To directly assess the role of Lzts2 in tumor susceptibility, we treated *Lzts2*-deficient mice with BBN to determine whether *Lzts2*-deficient mice are more susceptible to carcinogen-induced tumor development. We observed an increased incidence and more malignant phenotypes of BBN-induced bladder cancer in *Lzts2*-deficient mice in comparison with wild type littermates. Specifically, 6 of 26 Lzts2 null mice developed invasive transitional cell carcinomas, but none were found in heterozygous Lzts2 knock-out and wild type littermates. These data demonstrate that deletion of Lzts2 enhances the susceptibility of carcinogen-induced tumor development and progression. In a very similar study, Baffa *et al.* (26) reported that treatment of BBN resulted in carcinogen-induced bladder carcinoma in 82.3% of *Lzts1* heterozygous or 93.8% of homozygous knock-out mice *versus* only 8% of wild type control littermates, showing a higher incidence of BBN-induced bladder carcinomas in *Lzts1*-deficient mice than in *Lzts2*-deficient mice. Interestingly, higher incidences of spontaneous malignancies were also observed in *Lzts1*-deficient mice (3). These results suggest that *Lzts1*-deficient mice are more susceptible to spontaneous and BBN-induced bladder tumor development than *Lzts2* mice. More studies should be devoted to identifying the molecular mechanisms underlying these Lzts proteins in tumorigenesis.

The human *LZTS2* gene is located on chromosome 10 at 10q24.3, near 10q23.3, where PTEN, a tumor suppressor, was identified (4). Several lines of evidence suggest that more than one tumor suppressor may be harbored in this locus (5). However, no candidate gene has been identified within this region so far. Our current data provide a direct link between the deletion of Lzts2 and tumor development. Interestingly, we observed a relatively low penetrance of spontaneous malignancies in *Lzts2*-deficient mice. Additionally, BBN induction of urinary bladder carcinoma formation in *Lzts2*-deficient mice appears to be less effective than in Lzts1 knock-out mice. These data imply that other additional genetic and/or epigenetic changes may also be required in regulating Lzts2-mediated tumorigenesis. Thus, combinations of different mutations with Lzts2 deletion should be used in future studies to identify the additional factors and pathways that interact with Lzts2 in inducing tumor initiation and progression. Sequence analysis has shown that LZTS2 is highly similar to the tumor suppressor, LZTS1 (1). The *LZTS1* gene was mapped to chromosome 8p22, a region that is frequently deleted in human tumors (29). Therefore, it will be extremely interesting to investigate whether these two Lzts proteins are able to functionally compensate for each other in inducing oncogenic transformation using a compound knock-out mouse model.

The human *Lzts2* gene is located in the 10q24.3 region. This region has been frequently deleted in prostate cancer samples (1). Therefore, we examined the potentially abnormal LZTS2 expression in human tumor samples to assess the role of LZTS2 in human tumorigenesis. Using immunohistochemistry, we examined LZTS2 expression in prostate cancer tissue samples and observed decreased expression of LZTS2 proteins in human prostate cancer cells (Fig. 5), which elucidates a potential role of LZTS2 in human prostate cancer. In the past years, we spent significant effort to search for any genetic or epigenetic changes that may affect LZTS2 protein expression. However, we have not identified significant mutations or other abnormalities in the *LZTS2* gene locus from human prostate tumor samples. These negative findings suggest that the human LZTS2 gene may be a weak tumor susceptibility gene and require other susceptible gene loci for promoting tumor initiation and progression. This is also consistent with the low penetrance of spontaneous malignancies as we observed in *Lzts2*-deficient mice. Therefore, a combination of germ line mapping and an analysis of multiple alleles in specific imbalance and abnormality should be used in the future to further validate the role of LZTS2 as a tumor susceptibility gene.

We previously identified that LZTS2 is a novel β-catenin-interacting protein and regulates the cellular level, distribution, and activity of β-catenin (6). In this study, we further explored

the biological role of LZTS2 as a regulator of Wnt/β-catenin signaling. Using *Lzts2* null MEFs, we demonstrate that a loss of endogenous Lzts2 expression enhances cell proliferation and survival, which is consistent with the data in overexpression of LZTS2 protein in human prostate cancer cells. In this study, we also examined the effect of Wnt growth factors in Lzts2 null MEFs and observed a more pronounced effect of Wnt3a-conditioned medium in inducing cell growth and β-catenin-mediated transcription. Previous studies have shown that the nuclear shift of β-catenin reflects both an increase in total proteins and enhanced nuclear targeting that is regulated by the CRM/exportin nuclear export pathway (30–33). LZTS2 contains an intrinsic nuclear export signal and regulates the subcellular distribution of β-catenin through a CRM-dependent nuclear export signal (6). Using Lzts2 MEFs, we also assessed the effect of Lzts2 on the cellular localization of β-catenin. We observed more cytoplasmic staining of β-catenin in wild type MEFs than Lzts2 null MEFs (supplemental Fig. S1). These data are consistent with our previous observations in human tumor cells (6) and suggest that the biological roles of LZTS2 in regulating cellular β-catenin appear to be critical in both development and tumorigenesis. Previously, we reported that *Lzts2* null mice have severe kidney and urinary tract developmental defects, which are very similar to the abnormalities identified in β-catenin loss of function or gain of function mutations (34, 35). Dysregulated β-catenin cellular distribution and transcriptional activity has been suggested to be one underlying mechanism for the kidney defects in *Lzts2* null mice. Here, we further identified a tumor-prone phenotype in aged *Lzts2*-deficient mice. Interestingly, *Lzts1* null mice only displayed tumor susceptibility phenotypes (3). No renal defects or other abnormalities have been identified in this mouse model. These observations suggest that Lzts proteins may not functionally overlap with each other during the course of development, although they share a significant degree of sequence similarity. Future investigation of the potential interaction between Lzts1 and Lzts2 proteins in tumorigenesis wound be extremely interesting and should yield significant information regarding the regulatory role of Lzts proteins in oncogenic transformation.

REFERENCES

1. Cabeza-Arvelaiz, Y., Thompson, T. C., Sepulveda, J. L., and Chinault, A. C. (2001) LAPSER1. A novel candidate tumor suppressor gene from 10q24.3. *Oncogene* **20,** 6707–6717
2. Vecchione, A., Ishii, H., Shiao, Y. H., Trapasso, F., Rugge, M., Tamburrino, J. F., Murakumo, Y., Alder, H., Croce, C. M., and Baffa, R. (2001) Fez1/Lzts1 alterations in gastric carcinoma. *Clin. Cancer Res.* **7,** 1546–1552
3. Vecchione, A., Baldassarre, G., Ishii, H., Nicoloso, M. S., Belletti, B., Petrocca, F., Zanesi, N., Fong, L. Y., Battista, S., Guarnieri, D., Baffa, R., Alder, H., Farber, J. L., Donovan, P. J., and Croce, C. M. (2007) Fez1/Lzts1 absence impairs Cdk1/Cdc25C interaction during mitosis and predisposes mice to cancer development. *Cancer Cell* **11,** 275–289
4. Li, J., Yen, C., Liaw, D., Podsypanina, K., Bose, S., Wang, S. I., Puc, J., Miliaresis, C., Rodgers, L., McCombie, R., Bigner, S. H., Giovanella, B. C., Ittmann, M., Tycko, B., Hibshoosh, H., Wigler, M. H., and Parsons, R. (1997) PTEN, a putative protein tyrosine phosphatase gene mutated in human brain, breast, and prostate cancer. *Science* **275,** 1943–1947
5. Rasheed, B. K., McLendon, R. E., Friedman, H. S., Friedman, A. H., Fuchs, H. E., Bigner, D. D., and Bigner, S. H. (1995) Chromosome 10 deletion mapping in human gliomas. A common deletion region in 10q25. *Oncogene* **10,** 2243–2246
6. Thyssen, G., Li, T. H., Lehmann, L., Zhuo, M., Sharma, M., and Sun, Z. (2006) LZTS2 is a novel β-catenin-interacting protein and regulates the nuclear export of β-catenin. *Mol. Cell. Biol.* **26,** 8857–8867
7. Teufel, A., Weinmann, A., Galle, P. R., and Lohse, A. W. (2005) *In silico* characterization of LZTS3, a potential tumor suppressor. *Oncol. Rep.* **14,** 547–551
8. Hyun Hwa, C., Hye Joon, J., Ji Sun, S., Yong Chan, B., and Jin Sup, J. (2008) Crossregulation of β-catenin/Tcf pathway by NF-κB is mediated by Lzts2 in human adipose tissue-derived mesenchymal stem cells. *Biochim. Biophys. Acta* **1783,** 419–428
9. Schmeisser, M. J., Grabrucker, A. M., Bockmann, J., and Boeckers, T. M. (2009) Synaptic cross-talk between *N*-methyl-D-aspartate receptors and LAPSER1-β-catenin at excitatory synapses. *J. Biol. Chem.* **284,** 29146–29157
10. Sudo, H., and Maru, Y. (2007) LAPSER1 is a putative cytokinetic tumor suppressor that shows the same centrosome and midbody subcellular localization pattern as p80 katanin. *FASEB J.* **21,** 2086–2100
11. Sudo, H., and Maru, Y. (2008) LAPSER1/LZTS2. A pluripotent tumor suppressor linked to the inhibition of katanin-mediated microtubule severing. *Hum. Mol. Genet.* **17,** 2524–2540
12. Peng, Y., Clark, C., Luong, R., Tu, W. H., Lee, J., Johnson, D. T., Das, A., Carroll, T. J., and Sun, Z. (2011) The leucine zipper putative tumor suppressor 2 protein LZTS2 regulates kidney development. *J. Biol. Chem.* **286,** 40331–40342
13. Rodríguez, C. I., Buchholz, F., Galloway, J., Sequerra, R., Kasper, J., Ayala, R., Stewart, A. F., and Dymecki, S. M. (2000) High-efficiency deleter mice show that FLPe is an alternative to Cre-loxP. *Nat. Genet.* **25,** 139–140
14. Lakso, M., Pichel, J. G., Gorman, J. R., Sauer, B., Okamoto, Y., Lee, E., Alt, F. W., and Westphal, H. (1996) Efficient *in vivo* manipulation of mouse genomic sequences at the zygote stage. *Proc. Natl. Acad. Sci. U.S.A.* **93,** 5860–5865
15. Beliakoff, J., Lee, J., Ueno, H., Aiyer, A., Weissman, I. L., Barsh, G. S., Cardiff, R. D., and Sun, Z. (2008) The PIAS-like protein Zimp10 is essential for embryonic viability and proper vascular development. *Mol. Cell. Biol.* **28,** 282–292
16. Sharma, M., Li, X., Wang, Y., Zarnegar, M., Huang, C. Y., Palvimo, J. J., Lim, B., and Sun, Z. (2003) hZimp10 is an androgen receptor co-activator and forms a complex with SUMO-1 at replication foci. *EMBO J.* **22,** 6101–6114
17. Lin, D., Watahiki, A., Bayani, J., Zhang, F., Liu, L., Ling, V., Sadar, M. D., English, J., Fazli, L., So, A., Gout, P. W., Gleave, M., Squire, J. A., and Wang, Y. Z. (2008) *ASAP1*, a gene at 8q24, is associated with prostate cancer metastasis. *Cancer Res.* **68,** 4352–4359
18. Verras, M., and Sun, Z. (2006) Roles and regulation of Wnt signaling and β-catenin in prostate cancer. *Cancer Lett.* **237,** 22–32
19. Dull, T., Zufferey, R., Kelly, M., Mandel, R. J., Nguyen, M., Trono, D., and Naldini, L. (1998) A third-generation lentivirus vector with a conditional packaging system. *J. Virol.* **72,** 8463–8471
20. Farson, D., Witt, R., McGuinness, R., Dull, T., Kelly, M., Song, J., Radeke, R., Bukovsky, A., Consiglio, A., and Naldini, L. (2001) A new-generation stable inducible packaging cell line for lentiviral vectors. *Hum. Gene Ther.* **12,** 981–997
21. Verras, M., Brown, J., Li, X., Nusse, R., and Sun, Z. (2004) Wnt3a growth factor induces androgen receptor-mediated transcription and enhances cell growth in human prostate cancer cells. *Cancer Res.* **64,** 8860–8866
22. Peng, Y., Lee, J., Zhu, C., and Sun, Z. (2010) A novel role for protein inhibitor of activated STAT (PIAS) proteins in modulating the activity of Zimp7, a novel PIAS-like protein, in androgen receptor-mediated transcription. *J. Biol. Chem.* **285,** 11465–11475
23. Lakso, M., Sauer, B., Mosinger, B., Jr., Lee, E. J., Manning, R. W., Yu, S. H., Mulder, K. L., and Westphal, H. (1992) Targeted oncogene activation by site-specific recombination in transgenic mice. *Proc. Natl. Acad. Sci. U.S.A.* **89,** 6232–6236
24. Li, X., Thyssen, G., Beliakoff, J., and Sun, Z. (2006) The novel PIAS-like protein hZimp10 enhances Smad transcriptional activity. *J. Biol. Chem.* **281,** 23748–23756
25. Lubet, R. A., Huebner, K., Fong, L. Y., Altieri, D. C., Steele, V. E., Kopelov-

ich, L., Kavanaugh, C., Juliana, M. M., Soong, S. J., and Grubbs, C. J. (2005) 4-Hydroxybutyl(butyl)nitrosamine-induced urinary bladder cancers in mice. Characterization of FHIT and survivin expression and chemopreventive effects of indomethacin. *Carcinogenesis* **26,** 571–578
26. Baffa, R., Fassan, M., Sevignani, C., Vecchione, A., Ishii, H., Giarnieri, E., Iozzo, R. V., Gomella, L. G., and Croce, C. M. (2008) Fez1/Lzts1-deficient mice are more susceptible to *N*-butyl-*N*-(4-hydroxybutil) nitrosamine (BBN) carcinogenesis. *Carcinogenesis* **29,** 846–848
27. Weinstein, M. H., Signoretti, S., and Loda, M. (2002) Diagnostic utility of immunohistochemical staining for p63, a sensitive marker of prostatic basal cells. *Mod. Pathol.* **15,** 1302–1308
28. Lustig, B., Jerchow, B., Sachs, M., Weiler, S., Pietsch, T., Karsten, U., van de Wetering, M., Clevers, H., Schlag, P. M., Birchmeier, W., and Behrens, J. (2002) Negative feedback loop of Wnt signaling through upregulation of conductin/axin2 in colorectal and liver tumors. *Mol. Cell. Biol.* **22,** 1184–1193
29. Ishii, H., Baffa, R., Numata, S. I., Murakumo, Y., Rattan, S., Inoue, H., Mori, M., Fidanza, V., Alder, H., and Croce, C. M. (1999) The FEZ1 gene at chromosome 8p22 encodes a leucine-zipper protein, and its expression is altered in multiple human tumors. *Proc. Natl. Acad. Sci. U.S.A.* **96,** 3928–3933
30. Wiechens, N., and Fagotto, F. (2001) CRM1- and Ran-independent nuclear export of beta-catenin. *Curr. Biol.* **11,** 18–28
31. Staal, F. J., Noort, M., Strous, G. J., and Clevers, H. C. (2002) Wnt signals are transmitted through N-terminally dephosphorylated β-catenin. *EMBO Rep.* **3,** 63–68
32. Eleftheriou, A., Yoshida, M., and Henderson, B. R. (2001) Nuclear export of human β-catenin can occur independent of CRM1 and the adenomatous polyposis coli tumor suppressor. *J. Biol. Chem.* **276,** 25883–25888
33. Henderson, B. R. (2000) Nuclear-cytoplasmic shuttling of APC regulates β-catenin subcellular localization and turnover. *Nat. Cell Biol.* **2,** 653–660
34. Bridgewater, D., Cox, B., Cain, J., Lau, A., Athaide, V., Gill, P. S., Kuure, S., Sainio, K., and Rosenblum, N. D. (2008) Canonical WNT/β-catenin signaling is required for ureteric branching. *Dev. Biol.* **317,** 83–94
35. Moore, M. W., Klein, R. D., Fariñas, I., Sauer, H., Armanini, M., Phillips, H., Reichardt, L. F., Ryan, A. M., Carver-Moore, K., and Rosenthal, A. (1996) Renal and neuronal abnormalities in mice lacking GDNF. *Nature* **382,** 76–79